

Biases in total precipitable water vapor climatologies from Atmospheric Infrared Sounder and Advanced Microwave Scanning Radiometer

Eric J. Fetzer,¹ Bjorn H. Lambrigtsen,¹ Annmarie Eldering,¹ Hartmut H. Aumann,¹ and Moustafa T. Chahine¹

Received 18 August 2005; revised 17 January 2006; accepted 15 February 2006; published 26 April 2006.

[1] We examine differences in total precipitable water vapor (PWV) from the Atmospheric Infrared Sounder (AIRS) and the Advanced Microwave Scanning Radiometer (AMSR-E) experiments sharing the Aqua spacecraft platform. Both systems provide estimates of PWV over water surfaces. We compare AIRS and AMSR-E PWV to constrain AIRS retrieval uncertainties as functions of AIRS retrieved infrared cloud fraction. PWV differences between the two instruments vary only weakly with infrared cloud fraction up to about 70%. Maps of AIRS-AMSR-E PWV differences vary with location and season. Observational biases, when both instruments observe identical scenes, are generally less than 5%. Exceptions are in cold air outbreaks where AIRS is biased moist by 10–20% or 10–60% (depending on retrieval processing) and at high latitudes in winter where AIRS is dry by 5–10%. Sampling biases, from different sampling characteristics of AIRS and AMSR-E, vary in sign and magnitude. AIRS sampling is dry by up to 30% in most high-latitude regions but moist by 5–15% in subtropical stratus cloud belts. Over the northwest Pacific, AIRS samples conditions more moist than AMSR-E by as much as 60%. We hypothesize that both wet and dry sampling biases are due to the effects of clouds on the AIRS retrieval methodology. The sign and magnitude of these biases depend upon the types of cloud present and on the relationship between clouds and PWV. These results for PWV imply that climatologies of height-resolved water vapor from AIRS must take into consideration local meteorological processes affecting AIRS sampling.

Citation: Fetzer, E. J., B. H. Lambrigtsen, A. Eldering, H. H. Aumann, and M. T. Chahine (2006), Biases in total precipitable water vapor climatologies from Atmospheric Infrared Sounder and Advanced Microwave Scanning Radiometer, *J. Geophys. Res.*, *111*, D09S16, doi:10.1029/2005JD006598.

1. Introduction

[2] The Earth Observing System (EOS) satellites, flown by the National Aeronautics and Space Administration, each carry a suite of instruments for measurement of surface, ocean and atmospheric properties. This work compares total precipitable water vapor observations from two observing systems on the Aqua spacecraft: the Atmospheric Infrared Sounder (AIRS) experiment, and the Advanced Microwave Sounding Radiometer for EOS (AMSR-E). A primary objective of the EOS program is a climate quality data record extending over years to decades [King *et al.*, 1999; Parkinson, 2003]. One aspect of the observations from EOS is redundancy; for example, surface temperatures are measured nearly simultaneously by AIRS, AMSR-E and the Moderate Resolution Imaging Spectrometer (MODIS) on the Aqua spacecraft [Parkinson, 2003]. Other quantities measured by multiple

instruments on Aqua are cloud top properties and profiles of water vapor by MODIS and AIRS, and cloud liquid water by AMSR-E and MODIS. Instruments in NASA's A-Train satellite constellation, which includes Aqua, make additional redundant measurements [Stephens *et al.*, 2002]. For example, upper tropospheric water vapor is measured by both the Microwave Limb Sounder on Aura and by AIRS on Aqua; a preliminary intercomparison of these two data sets has been completed [Froidevaux *et al.*, 2006].

[3] While these redundant measurements suggest a wealth of information, a necessary first step in exploiting that information is reconciling similar observations. In this study we compare total precipitable water vapor (PWV) from AIRS and AMSR-E on Aqua. PWV was chosen for several reasons. Its high variability and relevance to hydrological processes makes it particularly appropriate for satellite monitoring. Also, the two instruments derive PWV independently. AIRS utilizes a combination of observed microwave and infrared radiances, while AMSR-E utilizes microwave observations alone. Since nonprecipitating clouds have little effect on microwaves at the frequencies employed by AMSR-E [O'Neill *et al.*, 2005], its PWV is

¹Jet Propulsion Laboratory, California Institute of Technology, Pasadena, California, USA.

ideally suited for diagnosing the effects of clouds on AIRS observations. Other advantages of AMSR-E for AIRS validation are its constant viewing angle and sensitivity to cloud liquid water and precipitation [Kawanishi *et al.*, 2003]. Insight into the effects of clouds on AIRS is relevant because AIRS retrieves height-resolved water vapor. Biases in AIRS PWV imply possible biases in AIRS profile water vapor climatologies.

[4] Several satellite instrument measured PWV prior to the launch of Aqua. The precursor to the AIRS experiment is the Television Operation and Infrared Optical Satellites (TIROS) Operational Vertical Sounder (TOVS) series of instruments. An operational microwave total water vapor sounder and predecessor to AMSR-E is the Special Sensor Microwave Imager (SSM/I) on the Defense Meteorological Satellite Program (DMSP) platforms. The TOVS, SSM/I and operational radiosonde water vapor observations have been merged into the NASA Water Vapor (NVAP) Project. Wittmeyer and von der Haar [1994], Randel *et al.* [1996] and Amenu and Kumar [2005] discuss the TOVS, SSM/I and operational radiosondes input to the NVAP product. Climatologies from these instruments have been intercompared extensively. As noted by Trenberth *et al.* [2005], PWV climatologies from different data sources can contain significant discrepancies.

[5] One important result of these comparisons is a global mean dry bias in the TOVS PWV observations relative to SSM/I [Wu *et al.*, 1993], but with wet biases in TOVS relative to SSM/I in regions of stratus clouds [Chaboureau *et al.*, 1998]. (Below we show similar results of global mean dry biases in AIRS relative to AMSR-E, and also that AIRS is wetter than AMSR-E in regions of stratus clouds.) The comparisons by Wu *et al.* [1993] and Chaboureau *et al.* [1998] are based on climatologies from separate satellites. Unlike the sensor pairs used in previous studies, AIRS and AMSR-E take observations coincident in time and collocated in space. We have over 130,000 daily matched AIRS and AMSR-E observations over water. We exploit this large, coincident and collocated data set to understand the effectiveness of the AIRS “cloud clearing” methodology, and show that clouds introduce only slight biases in AIRS PWV retrievals as a function of cloud amount, consistent with several other studies discussed below. We also utilize the direct matching between observations to make a detailed assessment of biases between the two observing systems as a function of location. That subset of observations with a one-to-one match between AIRS and AMSR-E allows us to determine observational biases: those seen when both instruments observe the same state. Observational biases are particularly important because they imply shortcoming in one or both observing systems. Systematic differences between AIRS and AMSR-E climatologies may also be due to sampling biases: those associated with each instrument observing a different ensemble of states. We hypothesize that the primary source of sampling biases is clouds affecting AIRS infrared signal; clouds prevent AIRS from sampling as complete a set of conditions as AMSR-E. Sampling biases have important implications for AIRS height-resolved water vapor, since its sampling biases, at least in the lowermost layers, are similar to those for PWV. We define a combination of sampling and observational biases to constitute the total bias.

[6] The remainder of this work is as follows: Section 2 describes the AIRS and AMSR-E observing systems, the known uncertainties of the two data sets, and the matchup methodology; section 3 presents the PWV climatology of the two periods of interest; section 4 shows the variations in yield of both instruments, including diurnal effects, and also how interinstrument observational biases vary with infrared cloud fraction retrieved by AIRS; section 5 shows AIRS yields and biases in PWV as a function of retrieved cloud amount; section 6 details the global variations in observational biases; section 7 shows the global variations in AIRS yields, and total biases between AIRS and AMSR-E; and section 8 presents summaries of results and concluding remarks.

2. Satellite, Instruments, Retrieval Methods, Quality Control and Data Matching

2.1. Aqua Spacecraft

[7] Launched on 4 May 2002, the Aqua satellite is in a near polar, Sun-synchronous orbit with equator crossing times of 0130 LT local time on the descending (southward moving) orbit, and 1330 LT on the ascending orbit. The Aqua orbital altitude is nominally 705 km, and its period is 98.8 min. Orbital correction maneuvers maintain the Aqua orbit with a repeat cycle of 16 days. The primary objective of the Aqua mission is a long-term record of the global hydrological cycle [Parkinson, 2003].

2.2. AIRS Experiment and Data Set

[8] The AIRS experiment consists of three distinct observing systems. The AIRS instrument is a 2378 channel nadir cross-track scanning infrared spectrometer with a 15 km field of view (FOV) [Pagano *et al.*, 2003]. Associated with AIRS are two microwave sounders: the Advanced Microwave Sounding Unit (AMSU) with a 45 km FOV, and the Humidity Sounder for Brazil (HSB) with a 15 km FOV [Lambrigtsen, 2003; Lambrigtsen and Calheiros, 2003]. The instruments became fully operational in September 2002. The AIRS system utilizes combined infrared and microwave observations [Suskind *et al.*, 2003]. The AIRS/AMSU/HSB instrument suite and retrieval algorithms [Aumann *et al.*, 2003] infers profiles of temperature and water vapor along with PWV, cloud and surface properties and minor gases up to total infrared cloud fraction (defined as the product of infrared emissivity and areal coverage) of about 70%. As shown below, the yield of retrievals utilizing both types of radiances is a rapidly decreasing function of infrared cloud fraction.

[9] The retrieved AIRS data are generated at the 45 km granularity of AMSU, utilizing a single AMSU spectrum and nine spectra each of AIRS and HSB (as appropriate) [Lambrigtsen and Lee, 2003]. The microwave observations contribute approximately 20 statistically independent pieces of information to a retrieval, while the infrared radiances contribute perhaps another 100 statistically independent pieces of information. (The exact information content of a single AIRS/AMSU/HSB radiance set is not known, though most of the approximately twenty thousand spectral observations are redundant.) We utilize PWV estimates generated by the version 4.0 AIRS retrieval algorithm [Fetzer *et al.*, 2005]. These data are currently available at the Goddard

DAAC at <http://disc.gsfc.nasa.gov/AIRS/index.shtml/>. This is the second publicly available AIRS data set; earlier version 3.0 data, with less complete quality flagging, have been available since August 2003 [Fetzer et al., 2003].

[10] The scan motor failed on HSB on 6 February 2003. Any water vapor climatology exploiting the entire AIRS record must take the loss of HSB into account, or utilize retrievals that exclude HSB from the entire record. The AIRS version 4.0 retrieved data are available both with HSB, when available, and without HSB.

[11] The AIRS V4.0 retrieval algorithm has several branching paths leading to solutions with varying information content. We use two AIRS quality flags in this study to distinguish fields of view with differing solutions. (Susskind et al. [2006] discuss the AIRS quality flags in more detail.) The first flag, designated *Qual_H2O*, indicates whether the microwave-only branch of the algorithm converged, and provides a total water vapor estimate. We consider here only those solutions with *Qual_H2O* = 0, or about 87% of the total. These are cases where the microwave-only part of the retrieval converges, while other cases are likely affected by microwave scattering by precipitation, leading to spurious results. A second flag indicates whether the infrared temperature profile retrieval algorithm converged. *Qual_Temp_Bot* indicates temperature retrieval convergence for the bottom-most part of the profile (*Qual_Temp_Bot* is never zero unless quality flags for the middle and top of the profile are also zero). Because the temperature solution from the infrared observations must converge for the water vapor solutions to proceed, the highest information content water vapor retrieval requires *Qual_Temp_Bot* = 0.

[12] We use the following terms to describe the two possible AIRS branching paths:

[13] 1. For partial retrieval, an AIRS/AMSU/HSB radiance set where the retrieval algorithm utilizes only the microwave observations for some part of a profile, while the retrieval using infrared (AIRS) radiances converges for some other part above the cloud tops. Partial retrievals become more frequent with increasing cloud amount, and are of lower information content. The quality flags for partial retrievals are *Qual_H2O* = 0 and *Qual_Temp_Bot* = 1.

[14] 2. For full retrieval, an AIRS/AMSU/HSB radiance set where complete convergence of the retrieval algorithm occurs, utilizing the full complement of microwave and infrared radiances. Only full retrievals have sufficient vertical resolution to characterize the distribution of water vapor to the specified system accuracy of 15% in 2 km layers over the entire profile. (AIRS sensitivity to water vapor drops rapidly around 100 hPa [Gettelman et al., 2004].) Full retrievals occur more frequently under less cloudy conditions; none are obtained for infrared cloud fractions greater than about 80%. The quality flags for full retrievals are *Qual_H2O* = 0 and *Qual_Temp_Bot* = 0.

[15] The fraction of full retrievals varies with season and location between about 10 and 90%. This is discussed more extensively below.

[16] Note that even the full retrieval solutions are obtained from a combination of microwave radiances (from AMSU and HSB) and infrared radiances (from AIRS). The microwave information is used primarily to for “cloud clearing” [see Susskind et al., 2003, and references therein],

or obtaining the cloud-free portion of the infrared scene. The microwave observations also contribute information about water vapor, with AMSU constraining the total and HSB constraining the profile. The infrared observations are needed for water vapor profiles with nominal 2 km resolution. In this study we require full retrievals to have this higher resolution over the entire profile. The currently configured AIRS/AMSU/HSB algorithm does not provide solutions for pure infrared (AIRS-only) observations. Any retrievals obtained from pure infrared observations will be even more strongly affected by clouds (i.e., biased in their sampling) than the full retrievals discussed below because the microwave observations add information to a properly configured retrieval. Also, while only full retrievals have complete, high-resolution water vapor profiles from the surface to ~100 hPa, some partial retrievals contain higher-vertical-resolution water vapor information at altitudes above the clouds tops. However, climatologies created from partial retrievals will have their own sampling biases, so the fundamental conclusion of this study holds: some portion of the water vapor field is unresolved by infrared observations, and the resulting biases are dependent upon the types of clouds present.

[17] The AIRS water vapor data have been validated in several studies. These studies consistently show biases of a few percent. Fetzer et al. [2003] presented full retrievals water vapor biases of -4 to 4% absolute, in 2 km layers between the surface and 500 hPa, against Vaisala operational radiosondes over water. Fetzer et al. [2004a] compared AIRS with European Center for Medium-range Weather Forecast (ECMWF) reanalyses in the Eastern Pacific, and operational radiosondes in Southern California and Hawaii, and showed biases of -5 to 3% absolute for full retrievals in the surface to 700 hPa layer. Susskind et al. [2006] compared AIRS retrievals against ECMWF fields and showed only slight variations in biases with cloud amount for several retrieved fields, including layer-resolved water vapor; we will show a similar result below for the AMSR-E PWV comparison. Divakarla et al. [2006] compared AIRS full retrievals against operational radiosondes and reported biases of less than about 10% absolute in 2 km layers against operational radiosondes. That analysis, however, included both land and water cases. L. M. McMillin et al. (Radiosonde humidity corrections and AIRS moisture data validation, submitted to *Journal of Geophysical Research*, 2005) used a combination of Global Positioning System (GPS) and radiosonde observations to validate AIRS water vapor profiles over land. Using GPS to normalize sonde profiles, they show agreement with AIRS profile water vapor to a few percent. The main conclusion of McMillin et al. is that AIRS is sufficiently stable and unbiased to reveal small diurnal differences in radiosonde sensitivity to water vapor. Tobin et al. [2006] compared AIRS retrievals against high-quality dedicated radiosondes launched for AIRS validation at the Atmospheric Radiation Monitoring (ARM) Tropical Western Pacific (TWP) site at Nauru (166.9°E, 0.5°S), and another ARM site in Oklahoma. Tobin et al. report biases at Nauru between AIRS and radiosonde water vapor in the range -4 to 6% absolute in 2 km layers in the lower troposphere, with weak dependence upon cloud amount. The PWV bias at Nauru is smaller than 5%. Tobin et al. characterize their results as

Table 1. Six Possible Cases Obtained For Every AIRS Field of View

	AIRS and AMSR-E Retrieval State
Case 1	AIRS partial retrieval and AMSR-E retrieval
Case 2	AIRS full retrieval and AMSR-E retrieval
Case 3	AMSR-E retrieval only
Case 4	AIRS partial retrieval only
Case 5	AIRS full retrieval only
Case 6	no AIRS retrieval and no AMSR-E retrieval

“AIRS retrievals for the tropical ocean TWP site have very good performance, with root-mean-square errors approaching the theoretical limit predicted by retrieval simulation studies;” that theoretical limit for PWV is 5% [Aumann *et al.*, 2003]. The Nauru result is particularly important for the tropical conditions discussed below. In summary, several comparisons of AIRS over-ocean full retrieval of water vapor against radiosondes consistently indicate mean biases of a few percent, with no significant dependence upon cloud amount. Note that none of these validation studies address AIRS sampling biases, as we do in this work.

2.3. AMSR-E Experiment and Data Set

[18] AMSR-E is a conically scanning microwave radiometer with a constant incidence angle of 55°. AMSR-E measures the dual polarization in six microwave bands centered between 6.925 and 89.0 GHz [Kawanishi *et al.*, 2003]. Over ocean surfaces AMSR-E measures PWV, cloud liquid water, surface wind speed, surface temperature, and ice concentration, while over land it measures soil moisture and snow water equivalent. AMSR-E retrieves precipitation amount over both water and land [Shibata *et al.*, 2003]. After launch, AMSR-E calibration was found to be compromised by indeterminate temperatures on the hot reference load, because of solar-induced thermal gradients. This required cross calibration with SSM/I and Tropical Rainfall Measurement Mission (TRMM) Microwave Imager instruments when Aqua orbits crossed those of the DMSP and TRMM satellites [Wentz *et al.*, 2003]. AMSR-E PWV is retrieved using regression on a large set of radiosondes [Wentz and Meisner, 2000]. The AMSR-E version 4 data are made available on a daily, quarter degree longitude-latitude grid from Remote Sensing Systems (www.remss.com); the observations themselves are taken at higher density [Kawanishi *et al.*, 2003], but averaged to the quarter-degree resolution [Shibata *et al.*, 2003].

[19] The AMSR-E PWV products have not been as extensively validated with radiosondes as PWV from AIRS. However, analyses to date show negligible bias. Szczodrak *et al.* [2006] describe comparisons of PWV observations from AMSR-E and ship-launched dedicated Vaisala RS80 and RS90 radiosondes. Those results encompass moist conditions in the Caribbean, typical summertime middle and high latitudes, and spring in the Mediterranean. Szczodrak *et al.* see “no obvious bias” between AMSR-E and radiosonde PWV, and RMS differences are 6% or less. They did not analyze their results as a function of cloud cover. The low biases given by Szczodrak *et al.* [2006] are consistent with the nature of the AMSR-E regression retrieval methodology described by Wentz [1997] and Wentz *et al.* [2003]. That algorithm uses a constantly updated set

of regression coefficients to ensure agreement between AMSR-E and operational radiosondes. Note in particular that the radiosonde set described by Wentz [1997] include many island locations at tropical through middle latitudes. These encompass virtually all of the climate regimes in the 50°S to 50°N range discussed later in this work.

2.4. Matching AIRS and AMSR-E Data

[20] The AIRS system provides 324,000 footprints per day (about 200,000 over water) at the spacing of the AMSU observations, nominally 45 km apart on swath 30 footprints wide. In this study, AMSR-E is matched to an AMSU FOV by selecting the AMSR-E gridded value nearest the geolocated FOV center. The temporal coincidence between collocated AIRS and AMSR-E observations is 3 min or less. Agreement between the two matched data sets is smaller than a few percent in almost all areas (as discussed below) suggesting that more refined matching is not necessary. Note, however, that this matching process does not include all AMSR-E observations, since the quarter-degree AMSR-E grid is roughly four times the density of the AMSU soundings, with their 50 km nominal spacing. We assume that the roughly 120,000 daily matched AMSR-E data matched to AIRS are a statistically representative sample of the entire AMSR-E observation set.

[21] The matches between AIRS and AMSU fall into six distinct cases determined by the output of the retrieval algorithms of the two instruments. These cases are described in Table 1. Note that only cases 1 and 2 allow direct comparison between AIRS and AMSR-E quantities. However, the other four cases 3–6 may contribute to climatologies generated from the two instruments. Case 3 in particular will be seen to significantly contribute to the AMSR-E means.

2.5. Periods of Comparison

[22] We consider two 16-day periods: 25 December 2002 through 9 January 2003 and 1–16 May 2003. We define a third situation of 25 December 2002 to 9 January 2003 with HSB. These two periods are roughly at the solstices, to give some interseasonal differences. Sixteen days is the repeat cycle of the Aqua orbit, so averaging over this period gives equal longitudinal coverage and even sampling.

3. Time-Mean Total Precipitable Water Vapor Maps

[23] The AMSR-E mean water vapor fields over cases 1–3 for 25 December 2002 to 9 January 2003 and 1–16 May 2003 are shown in Figures 1 and 2, respectively. All mapped data are placed on a grid with 5° resolution in longitude and latitude. Some of the largest changes between the two periods are indicative of a variety of atmospheric processes, with implications for both total and height-resolved water vapor. The largest changes between the two periods are at the western edges of ocean basins; the 10 kg/m² contour in 25 December 2002 to 9 January 2003 extends to about 30°N east of both Asia and North America, but is displaced from the map in 1–16 May 2003. (The units of kg/m² are equivalent to the commonly used millimeters.) Moistening is also seen in the northwestern Indian Ocean between the two periods. In the tropical Pacific Ocean the 60 kg/m²

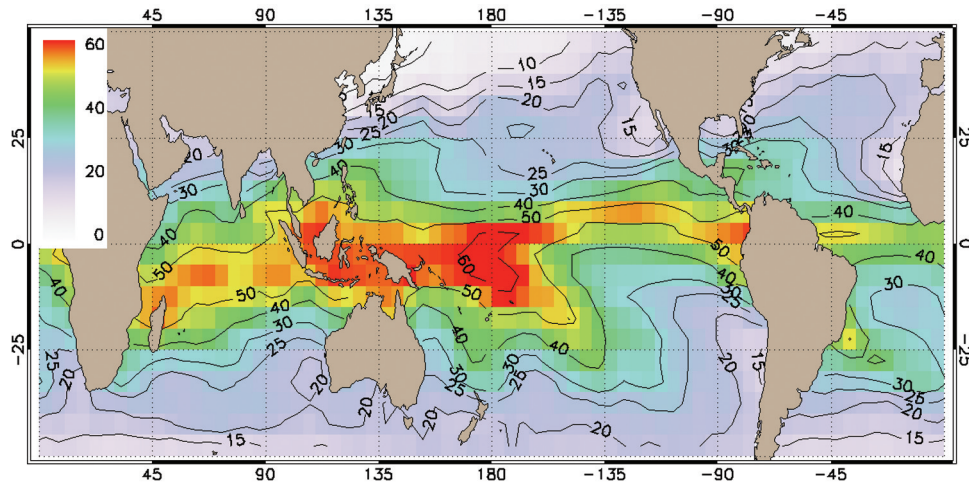


Figure 1. AMSR-E mean water vapor for 25 December 2002 to 9 January 2003. Contour interval is 5 kg/m^2 (equivalent to mm) up to 30 kg/m^2 and 10 kg/m^2 above that.

contour is displaced westward between boreal winter and spring, likely related to the shift in convective activity during the weakening El Niño of 2002–2003 [McPhaden, 2004]. Other areas experience little change in their total water vapor loading between 25 December 2002 to 9 January 2003 and 1–16 May 2003. For example, the 40 kg/m^2 contour in the eastern equatorial Pacific is nearly stationary, as is the 20 kg/m^2 contour off Baja California. The southern oceans near the bottom edges of Figures 1 and 2 show little change between 25 December 2002 to 9 January 2003 and 1–16 May 2003, similar to behavior in the northeast Pacific.

4. Variations in AIRS and AMSR-E Retrieval Yields

4.1. Global Yields

[24] Table 2 shows frequency of occurrence (yields) of the separate cases listed in Table 1 for the 25 December 2002 to 9 January 2003 with HSB, 25 December 2002 to 9 January 2003 and 1–16 May 2003. The global yield of

AIRS full retrievals (cases 2 and 5 combined) during 25 December 2002 to 9 January 2003 with HSB is 38%, and of partial retrievals (cases 1 and 4 combined) is 44%, while AMSR-E retrieval but no AIRS retrieval (case 3) occurs in 12% of scenes. Exclusion of HSB (25 December 2002 to 9 January 2003 with HSB versus 25 December 2002 to 9 January 2003) slightly increases the yield of full retrievals from 38 to 42%, while dropping the yield of partial retrievals to 41%. We will show later that the HSB loss leads to poorer agreement between AIRS and AMSR-E retrievals. The largest difference between 1–16 May 2003 and 25 December 2002 to 9 January 2003 globally is the increase in full retrieval yield from 42 to 47%, and a decrease in the fraction of pure AMSR-E footprints (case 3) from 14 to 11%. Situations with an AIRS retrieval but no AMSR-E retrieval (cases 4 and 5) compose 5–8% of the total. Only 1–2% of footprints contain no information at all (case 6). Maps of AIRS full retrieval yields are presented below in the discussion of biases.

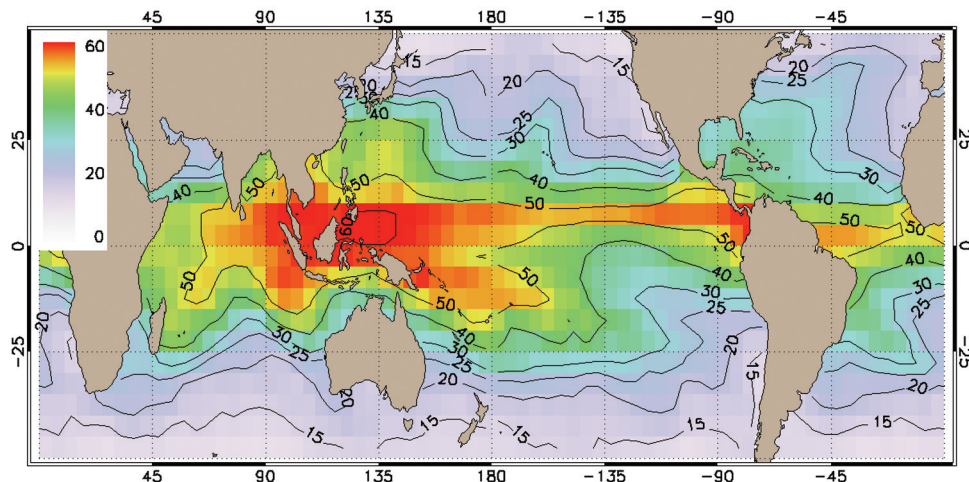


Figure 2. As Figure 1 but for 1–16 May 2003.

Table 2. Global Total Yields in Percent by Cases Described in for 25 December 2002 to 9 January 2003

	Case 1	Case 2	Case 3	Case 4	Case 5	Case 6	Total Counts
25 Dec. 2002 to 9 Jan. 2003 with HSB	41	35	12	4	3	2	2,081,022
25 Dec. 2002 to 9 Jan. 2003	37	38	14	4	4	2	2,084,485
1–16 May 2003	37	42	11	3	3	1	2,065,666

4.2. Diurnal Variation in Yields

[25] The Aqua orbit is Sun-synchronous with equator crossing times of 0130 LT southbound and 1330 LT northbound. These times are near the maxima and minima of many diurnally varying quantities, particularly clouds. As shown in Table 3 many of the global differences in retrieval yields just discussed are attributable to regional effects. The Western Pacific Warm Pool and the stratocumulus region off South America have diurnal changes in case 2 occurrence frequency of amplitude 3–9%. These are presumably associated with diurnal cycles in daytime cloudiness in deep and shallow convection. The largest diurnal amplitude of AIRS partial retrieval yields (case 1: from 51% during day to 71% at night) and lowest full retrieval yields (case 2: 8% at night) are seen over the northwest Pacific in winter. As will be seen below, conditions there present the greatest challenge to the AIRS retrieval system. However, such conditions are found over only a small fraction of the extratropical oceans.

5. Biases With Inferred Cloud Amount

[26] As Table 3 illustrates, the yield of directly matched AIRS and AMSR-E observations (cases 1 and 2 in Table 1) can vary considerably with location. Nevertheless, matched observations are useful in examining the AIRS retrieval methodology. Figure 3 compares AIRS and AMSR-E matched retrievals for period 25 December 2002 to 9 January 2003 with HSB, as a function of AIRS retrieved infrared cloud fraction. (As Table 2 shows, these represent 76% of total AIRS footprints). Figure 3 provides several insights, particularly into the AIRS retrieval technique. The root-mean-squared (RMS) differences between the two matched PWV data sets is about 0.2 kg/m². This agreement is better than the global mean different seen by *Amenu and*

Kumar [2005] between NVAP and a model reanalysis. This agreement suggests that both AIRS and AMSR-E retrieval methods are performing well since they use different methodologies to retrieve PWV. Note also the weak dependence of biases on inferred AIRS cloud amount. This is especially important for case 2 (solid red lines in Figure 3) indicating that the AIRS cloud clearing methodology [*Susskind et al.*, 2003] does not introduce significant cloud-dependent biases.

[27] Note also that Figure 3 shows that the AIRS infrared observations provide additional information to that in the microwave observations, though the effect is only about 2% in this case, as indicated by the lower RMS difference for case 2 (the dashed red lines in Figure 3). Finally, Figure 3 shows a day-night difference in AIRS relative to AMSR-E with a complex signature: the AIRS-AMSR-E biases are more positive during the day, but RMS differences are greater at night. This holds for both partial (case 1) and full (case 2) AIRS retrievals. The cause of this is not clear, though a combination of diurnal cycles in clouds and precipitation could be affecting all AIRS retrievals. (Recall that Table 3 showed a detectable day-night difference in retrieval yields in several regions.) This diurnal effect is only about 1 kg/m². *Dai et al.* [2002] compared the diurnal cycle in radiosondes and GPS receivers and saw a diurnal amplitude of 1.8 kg/m² over the Great Plains of the United States. Note that the amplitude of the diurnal difference in Figure 3 is comparable for full (solid red curves) and partial retrievals (solid blue curves).

[28] Statistics of differences in AIRS and AMSR-E PWV for the same conditions as for Figure 3, but for AIRS retrievals without HSB, are shown in Figure 4. Comparing Figure 3 with Figure 4 shows that HSB does provide information about PWV for conditions where AIRS and AMSR-E have matching observations (cases 1 and 2). The

Table 3. Occurrence Frequencies in Percent by Case as Described in Table 1, for Three Regions in the Indo-Pacific Region^a

	Case 1	Case 2	Case 3	Case 4	Case 5	Case 6
<i>Southwest Pacific</i>						
25 Dec. 2002 to 9 Jan. 2003 with HSB	54/65	22/14	12/15	6/2	2/0	1/0
25 Dec. 2002 to 9 Jan. 2003	51/60	24/19	13/16	6/2	2/0	1/0
1–16 May 2003	36/47	50/27	8/9	2/7	1/6	0/1
<i>Warm Pool</i>						
25 Dec. 2002 to 9 Jan. 2003 with HSB	42/37	31/34	14/12	4/5	3/5	3/3
25 Dec. 2002 to 9 Jan. 2003	38/34	32/35	18/15	3/5	3/5	3/4
1–16 May 2003	39/36	38/45	13/11	3/2	3/2	2/2
<i>Northwest Pacific</i>						
25 Dec. 2002 to 9 Jan. 2003 with HSB	51/71	15/8	16/10	9/5	2/1	4/2
25 Dec. 2002 to 9 Jan. 2003	48/65	17/14	17/10	8/5	2/1	4/2
1–16 May 2003	45/43	23/22	24/28	2/2	1/0	2/2

^aRegions are as follows: Southwest Pacific: South America-100°W and 0–30°S; Warm Pool: 90–180°E and 15°S–15°N; Northwest Pacific: Asia-180°E and 30–50°N, for 25 December 2002 to 9 January 2003. Pairs represent means for daytime (ascending)/nighttime (descending) orbits.

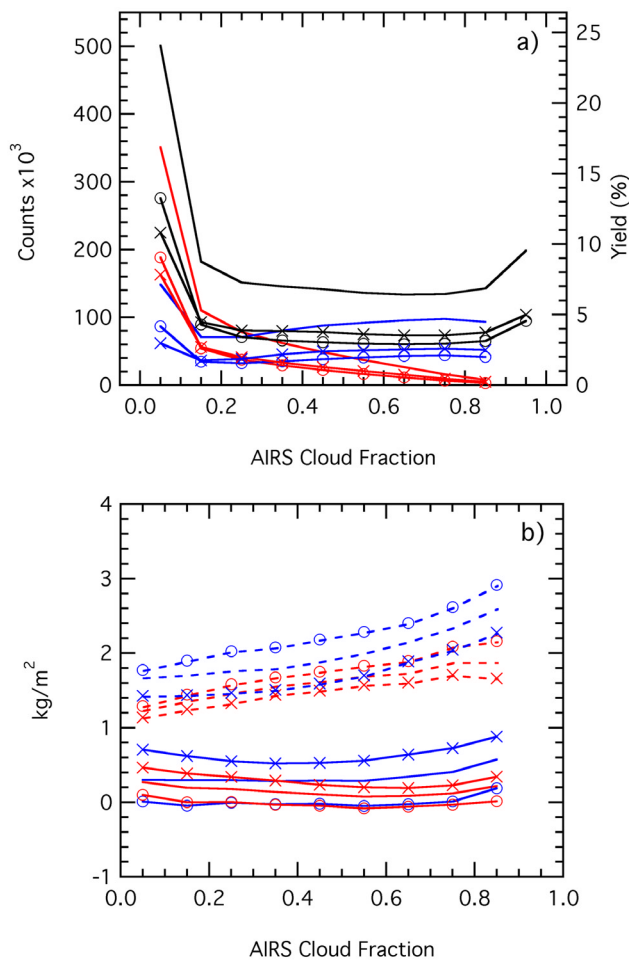


Figure 3. (a) Yields of AMSR-E (black), and AIRS retrievals, in thousands and as percent of total, and (b) mean (solid) and root-mean-squared (dashed) differences between AIRS and AMSR-E in kg/m^2 . Blue and red indicate AIRS values for case 1 and case 2, respectively, in Table 1; daytime is shown as circles, night is shown as crosses, and day/night combined are shown without symbols.

biases in PWV from AIRS relative to AMSR-E are as large as $1.8 \text{ kg}/\text{m}^2$ without HSB, but under $1 \text{ kg}/\text{m}^2$ with HSB. The RMS differences grow with retrieved cloud amount, though the change is only from about 1.5 to $2.5 \text{ kg}/\text{m}^2$. The diurnal amplitudes in Figure 4 are roughly the size of those in Figure 3.

[29] The diurnal effects shown here are interesting, but they are relative measurements from two instruments, each potentially affected by natural diurnal variability. Clouds reduce coverage by AIRS, while precipitation reduces coverage by AIRS and AMSR-E. Clouds and precipitation both have diurnal cycles, so the diurnal differences shown here may be caused by diurnal modulation of both instruments' sampling. This effect must be considered in any diurnal cycle PWV climatology from either instrument.

[30] The previous two figures show small, AIRS-AMSR-E PWV observational biases varying weakly with cloud amount up to 80% infrared cloud fraction where AIRS full retrieval yields drop to zero. We performed analogous comparisons to those described for Figures 3 and 4 over

several limited regions, including the equatorial belt, the tropical Western Pacific, the midlatitude storm tracks, the northeast and northwest Pacific, and the region off Peru. In all regions the AIRS-AMSR-E PWV observational biases are small and weakly varying with cloud amount, similar to Figures 3 and 4. This is consistent with AIRS-radiosonde [Tobin *et al.*, 2006; Divakarla *et al.*, 2006] and AIRS-ECMWF [Suskind *et al.*, 2006] validation comparisons discussed previously. (A several percent increase in RMS differences with cloud amount is also consistent with those results.) Also, the AMSR-E PWV estimates are constrained by a regression retrieval using a large number of operational radiosondes from oceanic islands [Wentz, 1997], minimizing AMSR-E PWV biases for all cloud amounts. These considerations all support a fundamental assumption of this study: AMSR-E observational biases contribute only a few percent to AIRS-AMSR-E total biases that will be seen below to range from -30 to $+70\%$.

6. Observational Biases With and Without HSB

[31] The HSB instrument is an important component of the AIRS experiment. As will be shown, its loss introduces

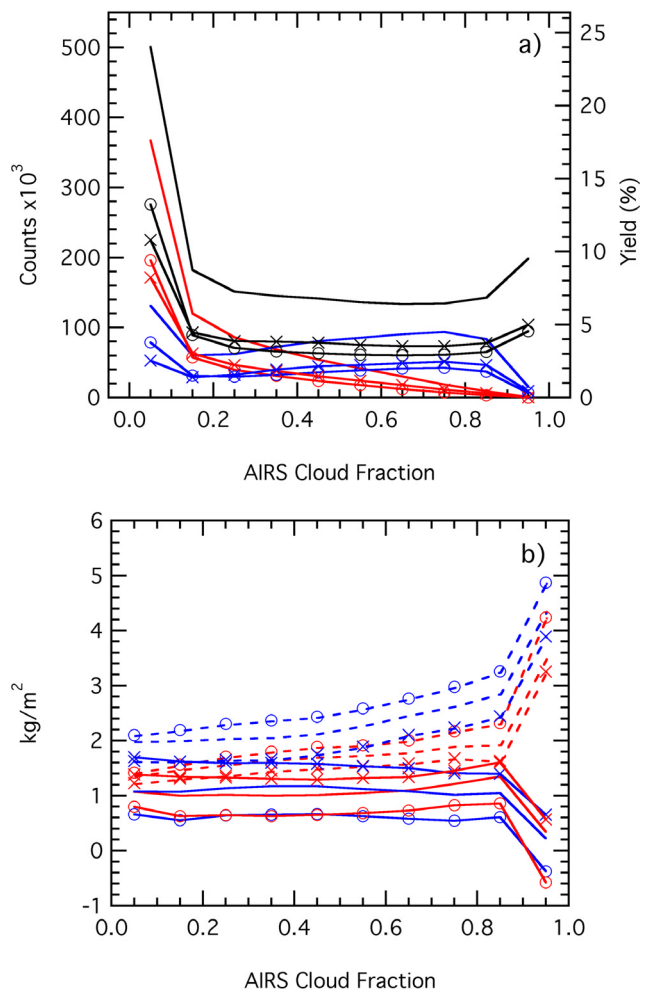


Figure 4. (a and b) As Figure 3 but for AIRS retrievals without HSB.

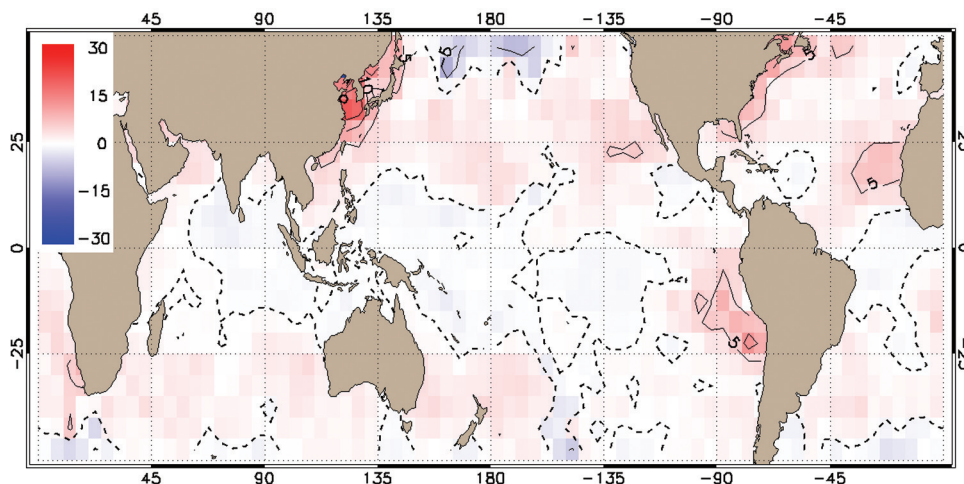


Figure 5. Percent difference between AIRS and AMSR-E mean PWV, relative to AMSR-E mean PWV, for full retrievals (case 2 in Table 1), with HSB included, for 25 December 2002 to 9 January 2003. Contour interval is 5%, and the zero contour is dashed.

moist observational biases into the PWV fields from AIRS (as defined above, observational biases occur when both instruments infer different PWV in the same view). Figure 5 shows the fractional difference between AIRS and AMSR-E for matched cases defined as:

$$\text{Difference} = 100 \times \frac{\langle PWV_{\text{AIRS}} \rangle - \langle PWV_{\text{AMSR-E}} \rangle}{\langle PWV_{\text{AMSR-E}} \rangle} \quad (1)$$

Here the angle brackets signify a time mean over the grid box. Figure 5 shows the differences for AIRS full retrievals with HSB; it was generated using matched cases only (case 2 in Table 1). The relative differences in Figure 5 are within the range $\pm 5\%$ over most of the globe, with AIRS slightly drier in the north Pacific. The global RMS difference for all the points in Figure 5 is 5%. This is also the AIRS/AMSU/HSB measurement specification for PWV [Aumann *et al.*, 2003], and close to the performance limits of the AIRS system [Suskind *et al.*, 2003]. This excellent agreement suggests that both AIRS and AMSR-E are performing well when case 2 in Table 2 prevails. In particular, this is confirmation that the AMSR-E cross-satellite calibration described by Wentz *et al.* [2003] is effective.

[32] Figure 6 shows the corresponding differences for retrievals without HSB. Retrievals without HSB have wet biases relative to AMSR-E of up to 30% in the northwest Atlantic and Pacific Oceans. These regions are characterized by cold air outbreaks: cold, dry air masses of continental origin moving over relatively warm ocean water. These are also regions of persistent low stratus during winter [Norris, 1998; Klein and Hartmann, 1993]. Conditions there often lead to small vertical-scale structure not as resolvable by AIRS/AMSU compared to the full AIRS/AMSU/HSB suite. These conditions include a shallow moist layer under a deep, cold, very dry layer [Fetzer *et al.*, 2004b]. Furthermore, the AIRS full retrieval yield in this region can be as small as 8% (see Table 2). A likely explanation for much smaller observational biases for 25 December 2002 to 9 January 2003 with HSB is the increased information about vertical water vapor structure from HSB. HSB has

four height-dependent channels to constrain the water vapor vertical distribution [Lambrigtsen and Calheiros, 2003], while AMSU has a single channel to constrain PWV [Rosenkranz, 2003]. The additional information in the HSB radiances improves the AIRS PWV solution under the rather extreme conditions encountered in cold air outbreaks. A similar, though less dramatic effect of the loss of HSB is seen in the southeast Pacific Ocean off Peru, where regions of subsidence lead to extensive fields of subtropical stratus.

[33] In addition to the effect of HSB on observational biases, two other conclusions can be drawn from this comparison. First, much of the global moist bias in AIRS retrievals without HSB as a function cloud amount (see Figures 3 and 4) is associated with regions of cold air outbreaks. Second, the loss of HSB will affect any height-resolved climatology generated from the AIRS/AMSU/HSB system, especially in the north Atlantic and Pacific oceans during winter and, to a lesser extent, in subtropical stratus regions.

7. Total Biases in AIRS Full Retrievals

[34] An appropriate comparative climatology between AIRS and AMSR-E will not be based on matched FOVs only, as describe above. Instead, it will utilize all AMSR-E observations regardless of the state of the AIRS retrieval. Here we describe biases between PWV climatologies from AIRS full retrievals and from AMSR-E. As described above, these are total biases, unlike the pure observational biases described in previous discussions.

[35] The most important insights from AIRS water vapor concerns not PWV, but water vapor profiles; PWV has been well observed from space for decades [Randel *et al.*, 1996; Amenu and Kumar, 2005], while AIRS is generating the highest-vertical-resolution satellite water vapor data set yet available, with resolution of roughly 2 km vertically [see Tobin *et al.*, 2006; Divakarla *et al.*, 2006]. Given the importance of AIRS water vapor profiles, we use AMSR-E to assess biases in AIRS full retrievals of water vapor.

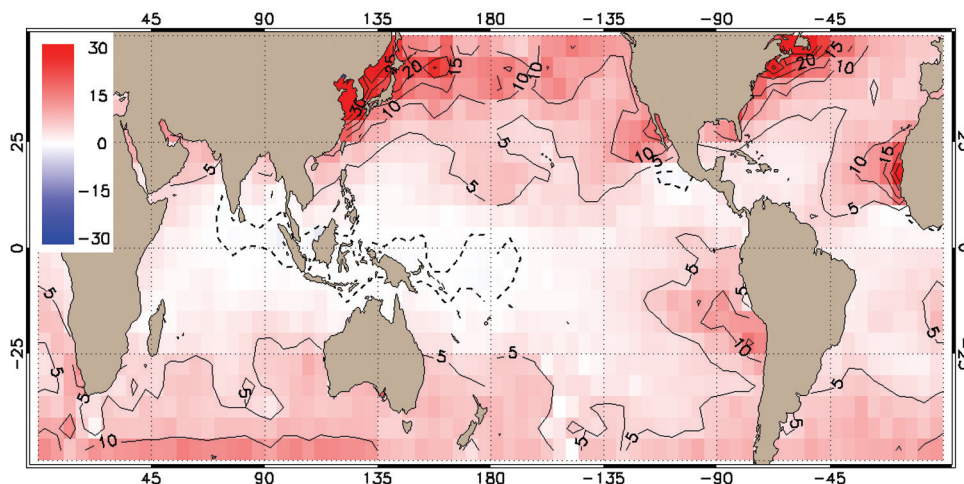


Figure 6. As Figure 5 but for AIRS retrievals without HSB.

Those regions with biases in PWV will likely also have biases in some, or all, of the water vapor profile. The height distribution of those biases is dependent upon the cloud fields, and is a topic for future research.

[36] Figure 7 shows the yield of AIRS full retrievals for 25 December 2002 to 9 January 2003 with HSB. Figure 7 is a more detailed picture of the yields shown for case 2 in Tables 2 and 3. The subtropical belts away from the continents have the highest yields, exceeding 90%. Lowest yields of less than 15% are seen in the northwest Pacific and Atlantic Oceans, and also in subtropical stratus cloud regions to the immediate west of continents. Another yield minimum is seen on and to the north of the equator in the Pacific, and is likely associated with higher clouds in the Intertropical Convergence Zone (ITCZ). The associated map for 25 December 2002 to 9 January 2003 (no HSB retrievals) is qualitatively very similar to Figure 7.

[37] Figure 8 shows the total relative bias between AIRS full retrievals and AMSR-E for 25 December 2002 to 9 January 2003 with HSB, relative to AMSR-E. Moist total biases for AIRS are seen in either subtropical stratus belts

west of the continents or downwind of Asia and North America, while dry total biases are seen in most other regions. The biases in Figure 8 vary between about -30 and $+70\%$. These should be compared with the known observational biases against radiosondes (less than 5%) discussed in section 2, and the relative observational biases ($\sim 5\%$ in most regions) shown in Figure 5. The discrepancy between low observational biases and high total biases is most plausibly explained by differences in the sampling characteristics of AIRS and AMSR-E. This is discussed in more detail in the conclusions.

[38] AIRS has the largest dry biases in Figure 8 in the region of persistent high-level to midlevel cloudiness, most notably the high-latitude belts, but also in the ITCZ. Figure 8 shows clearly that the AIRS total biases relative to AMSR-E can be of either sign, with regions of low-level clouds introducing a wet bias while regions of higher clouds introduce a dry bias. We hypothesize that these differences can largely be explained by the reduction of AIRS full retrieval coverage with increasing cloud cover. Consider the region of largest AIRS wet bias to

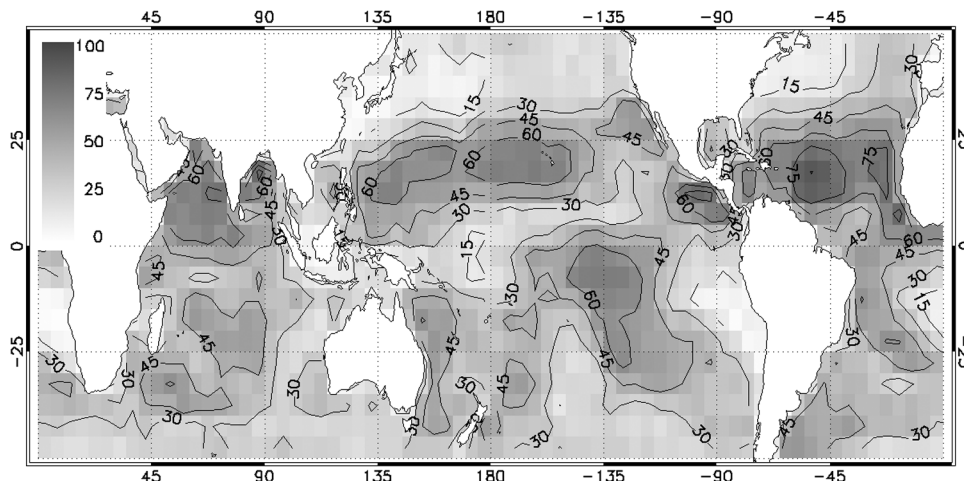


Figure 7. AIRS full retrieval yield (in percent) for 25 December 2002 to 9 January 2003 with HSB. Yield of 100% represents roughly three to five thousand counts per bin.

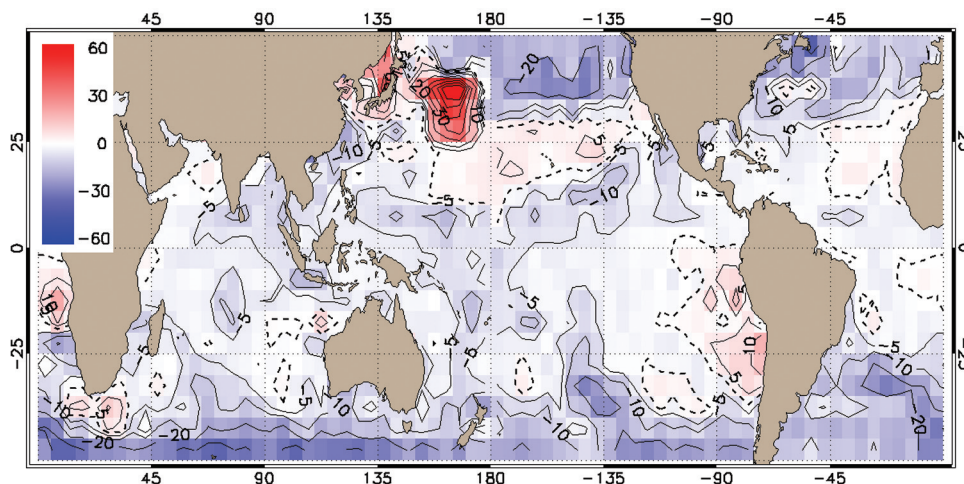


Figure 8. AIRS-AMSR-E PWV total biases during 25 December 2002 to 9 January 2003, as percent of AMSR-E mean, for AIRS full retrievals with HSB included. Contour interval is 5% up to 30% absolute value and 10% above that. The zero contour is dashed.

the south and east of Japan in Figure 8. This region is characterized by persistent low-level clouds overlain by a thick, cold and dry layer during frequent cold air outbreaks from Siberia [Fetzer *et al.*, 2004b]. That persistent cloudiness prevents AIRS full retrievals at those times when the atmosphere is relatively very dry. However, this region also experiences periods of reduced cloudiness when humid oceanic air masses from the subtropics move through. During those times AIRS full retrieval yields may be as high as 75%, as suggested by Figure 7. This less cloudy subtropical air is much more moist than air moving off the Asian continent. Consequently, AIRS full retrievals preferentially sample drier conditions in the wintertime midlatitude western Pacific. In contrast, in the extratropical eastern Pacific, midlatitude storm systems bring a combination of cloud cover and above-average water vapor loading. During these times AIRS full retrieval yields are very low. Between storms in the eastern Pacific, however, high-pressure ridges and polar air masses moving southward often dominate the flow. Those drier conditions lead to large areas of scattered shallow convective clouds where the AIRS full retrieval yield is high. This mechanism explains why AIRS samples drier conditions preferentially in regions of midlatitude storm systems.

[39] The most important conclusion to be reached from Figure 8 is that the AIRS total biases depend upon the meteorology of the region being observed. In regions of cold air outbreaks or subtropical stratus, clearer conditions tend to be moister, leading to a moist bias in the AIRS full retrievals. In regions of midlatitude storms, clearer conditions tend to be drier, leading to dry biases in AIRS full retrievals. Low retrieval yields do not necessarily lead to a large bias between AIRS and AMSR-E PWV, however. In the tropical Pacific, yields in Figure 8 can be as low as 15%, but the biases in Figure 8 are only a few percent. This suggests that deep convective clouds have little effect on AIRS full retrieval sampling.

[40] Earlier studies have noted biases in the TOVS PWV climatologies. Wu *et al.* [1993] note likely dry sampling biases at high latitudes analogous to those shown here, and suggest they are due to cloud-induced sampling. Similarly,

Chaboureau *et al.* [1998] attribute moist biases between TOVS and SSM/I climatologies in stratocumulus regions to clouds modulating the TOVS sampling. Those previous data sources are more limited in their information about cloud cover, while the combined Aqua instrument suite of AIRS, AMSR-E and MODIS make detailed, simultaneous cloud observations. Therefore the effects of clouds on AIRS retrievals can be stated as hypotheses, testable as climatologies of AIRS water vapor conditional upon cloud state.

[41] As a comparison of observational biases in Figure 5 and total biases in Figure 8 shows, the observational biases contributes only slightly to the total biases. Notable exceptions are over the northwestern-most Pacific and Atlantic oceans, where cold air outbreaks are most intense. Note that this result pertains to conditions with HSB in the retrievals (25 December 2002 to 9 January 2003 with HSB).

[42] The total AIRS-AMSR-E biases for full retrievals without HSB are shown in Figure 9. Qualitatively this is very similar to the result for 25 December 2002 to 9 January 2003 with HSB shown in Figure 8. However, the regions of moist biases in Figure 9 are more extensive, with larger extrema. Note in particular that the subtropical stratus cloud regions to the west of the continents experience increased wet biases without HSB. The loss of HSB leads to an increase in the wet biases in stratus regions by 5–10% or greater, with the most pronounced change immediately adjacent to land, where stratus clouds are also most prevalent. This conclusion has important implications for any long-term height-resolved water vapor climatology from AIRS in these regions, as in the work by Fetzer *et al.* [2004a].

[43] Further comparison of Figures 8 and 9 shows one unexpected result: the loss of HSB gives better agreement between AIRS and AMSR-E in the high-latitude storm tracks. The maxima in the northeast Pacific, south Atlantic and along the southernmost margins are all less negative in Figure 9 than Figure 8.

[44] Figure 10 shows the yield for 1–16 May 2003, complementary to the boreal winter yields of Figure 7. As in northern winter, the May yields are lowest in extratrop-

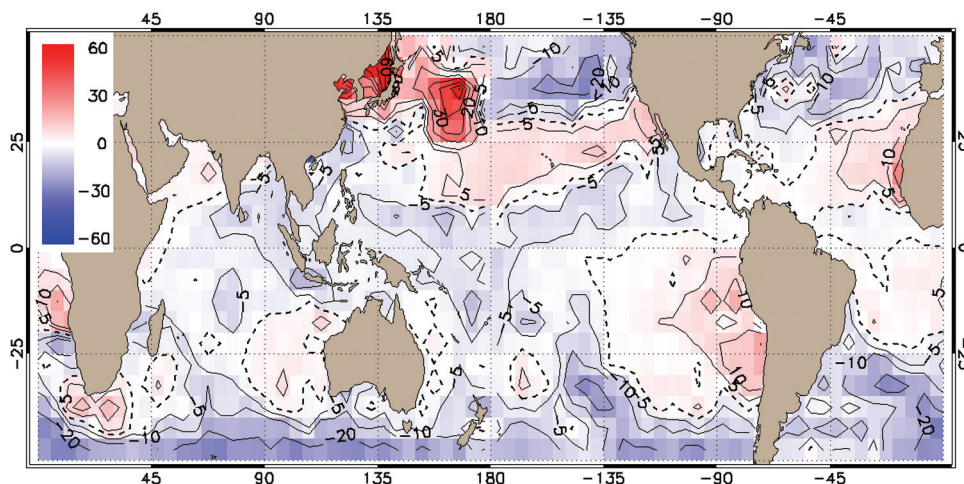


Figure 9. AIRS-AMSR-E total bias, as in Figure 8 but for AIRS full retrievals without HSB.

ical storm belts and subtropical stratus regions. The local minimum in the western Pacific Warm Pool is not as pronounced in May as in northern winter, and the global maxima have moved from the northern subtropics to the southern subtropics. As in northern winter (compare Figure 7), the highest yields are in the subtropical trade cumulus belts in the winter hemisphere. Lowest yields in May are seen to the west of Baja California, likely associated with climatologically persistent stratocumulus clouds. Figure 10 shows no evidence of the very low yields seen in Figure 7 to the east of the winter continents. This is consistent with a lack of paths across southern continents for air masses moving from polar to subtropical latitudes, as with Asia and North America during winter.

[45] Figure 11 shows the biases between AIRS full retrievals and AMSR-E for 1–16 May 2003 (analogous to the northern winter conditions in Figure 8). The most significant feature in Figure 11 is the large dry biases at far northern latitudes, evidence that the midlatitude storm systems hypothesized to lead to dry biases in AIRS are now confined to the highest latitudes. The largest wet bias is seen off Baja California, in the vicinity of the low yields discussed above. As with the wintertime biases shown in

Figure 8, the majority of the planet’s ocean regions have small observational biases between AIRS and AMSR-E.

8. Summary and Conclusions

[46] We analyzed AIRS and AMSR-E total precipitable water vapor (PWV) over oceans between 60°S and 60°N for one 16-day period in boreal winter 2002–2003, and a second 16-day period in May 2003. The first part of this work compared matched AIRS and AMSR-E total water vapor retrievals as a function of inferred AIRS cloud amount. The AIRS yields declined significantly as a function of cloud amount. The biases and RMS differences were only weak function of AIRS retrieved infrared cloud fractions, however. Also, the AIRS PWV observations utilizing both microwave and infrared radiances (full retrievals) showed better agreement with AMSR-E than those utilizing microwave radiances alone (partial retrievals). This implies that the infrared radiances improved the water vapor estimate by a few percent. Those infrared channels are critical to resolving the water vapor profile, however. We also showed that the loss of HSB changed the global mean

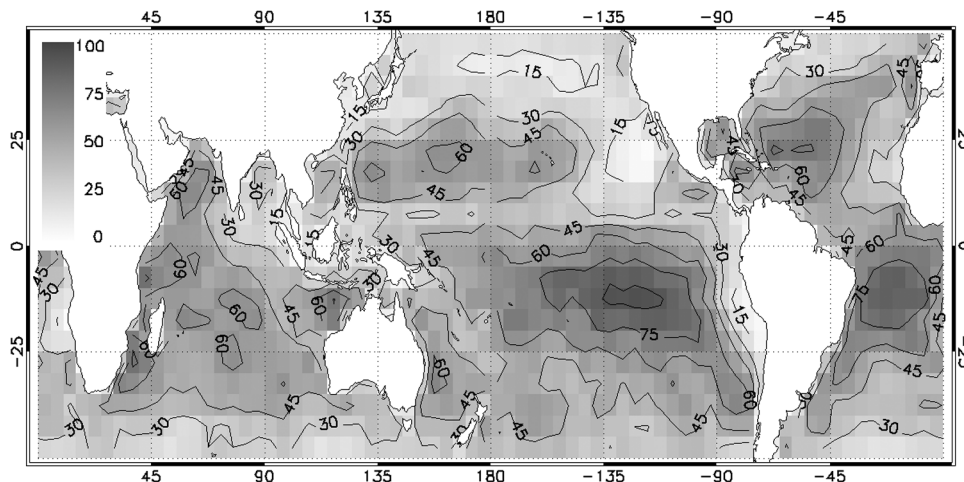


Figure 10. AIRS full retrieval yield, as in Figure 7 but for 1–16 May 2003.

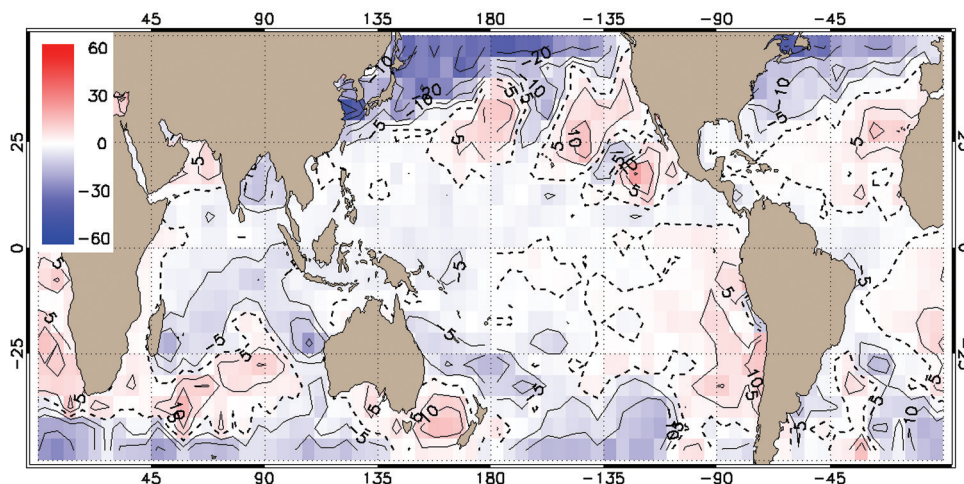


Figure 11. AIRS-AMSR-E total bias, as in Figure 5 but for 1–16 May 2003.

PWV biases slightly, with AIRS/AMSU retrievals being slightly wetter than AIRS/AMSU/HSB retrievals.

[47] The second part of this work looked at comparative climatologies from AIRS and AMSR-E for two periods, and also examined the effect of the loss of HSB on their relative biases. We considered only AIRS full retrievals, those utilizing a combination of infrared and microwave radiances. These are the retrievals with sufficient vertical resolution to describe height-dependent water vapor climatologies. Two types of biases are examined: observational biases, when both instrument sample the same atmospheric state, and, total biases, hypothesized to be due mainly to AIRS observing a less complete set of states because of the effects of intervening clouds. The complete AIRS/AMSU/HSB system had RMS sampling differences in PWV against AMSR-E meeting the measurement specification of the AIRS, or about 5%. Observational biases were less than 5% for all but a few, small regions in the wintertime northern hemisphere. The loss of HSB leads to wet observational biases in AIRS. The observational biases without HSB can be as great as 25%, though these largest values are seen only in very limited regions in cold air outbreaks from Asia and North America. Retrievals with and without HSB also showed wet observational biases of <5 and 5–10%, respectively, in the subtropical stratus belts. These largest AIRS wet observational biases are apparently related to stratus cloud cover, since stratus prevails both in cold air outbreaks and in subtropical eastern ocean basins. Wet observational biases of a few percent were also seen in high-latitude and midlatitude storm belts. Somewhat surprisingly, the observational biases in AIRS at higher latitudes

were reduced with the loss of HSB, though this may be a spurious result. All regions with observational bias absolute values of 10% or more also had AIRS full retrieval yields of only 10–20%. Most other climate regimes showed little or no observational bias. Notably, trade wind cumulus regions had observational biases between AIRS and AMSR-E near zero and AIRS full retrieval yields as high as 90%.

[48] The third part of this work examined total biases between AIRS and AMSR-E. Total biases are caused by a combination of observational bias and different sampling by the two instruments. Table 4 summarizes the total biases between AIRS and AMSR-E, and the AIRS retrieval yields for several dominant climate regimes over ocean. In high latitudes, AIRS full retrievals consistently gave dry total biases of about 30% despite slight moist observational biases. We hypothesize the total bias to be due to the correlation between cloudiness, high PWV, and lower full retrievals yields in high-latitude storms; this effect overwhelms any inherent wet observational biases. In contrast, in stratus regions a slight moist AIRS observational bias reinforces a moist sampling bias. We hypothesize that the moist total biases in stratus regions are also due to the effect of clouds on AIRS sampling. In contrast to midlatitude storm systems, heavy stratus cover is associated with a moist, shallow boundary layer and very dry overlying atmosphere [Stevens *et al.*, 2003], giving low PWV. This cloud cover is disrupted by either deeper convection [Pyatt *et al.*, 2005] or prefrontal moisture transport [Iskenderian, 1995; Ralph *et al.*, 2004]. So, in stratus belts lower cloudiness is more likely associated with higher PWV amounts. Thus the sampling biases reinforce the inherent wet observational bias of AIRS in stratus regions. This effect is exacerbated by the loss of HSB, by 5–10%. The most pronounced sampling bias is seen in 25 December 2002 to 9 January 2003 to the south and east of Japan. A strong gradient in observational biases, and a very large maximum wet total bias near 70% is seen there. We ascribe this to an analogous but more pronounced effect as described above for subtropical stratus regions. Off Japan conditions are either heavy stratus with very dry overlying air, or, clearer and more moist conditions from subtropical air masses [Fetzer *et al.*, 2004b]; these conditions lead to a very wet total bias for AIRS. Total biases are quite small in

Table 4. Summary of AIRS-AMSR-E Total Biases, Relative to AMSR-E Means, and AIRS Full Retrieval Yields, for Typical Ocean Climate Regimes and Retrievals Without HSB

Climate Regime	AIRS-AMSR-E Total Bias, %	AIRS Full Retrieval Yields, %
Midlatitude storm belts	–10 to –30	15 to 30
Cold air outbreaks	+30 to +70	<15
Subtropical stratus	–5 to –15	<15
Trade wind cumulus	–5 to +5	50 to 90
Tropical deep convection	–5 to +5	15 to 50

most other regions, with values of only a few percent throughout most of the tropics and subtropics. Yields in the equatorial regions can be as low as 15%, implying heavy cloud cover, but the biases there are a few percent. This implies that tropical deep convection includes yet a third class of cloud types, leading to reduced AIRS yields but only small sampling biases in PWV against AMSR-E. Low total biases between AIRS and AMSR-E in equatorial regions, between AIRS and sondes at the ARM TWP site at Nauru [Tobin *et al.*, 2006], and between AMSR-E and Caribbean sondes [Szczodrak *et al.*, 2006] all indicate good performance by both satellite systems in regions of deep convection. Importantly, the microwave information in AMSR-E and AMSU/HSB appears sufficient to identify scenes with large amounts of cloud ice. Those scenes are not, on average, significantly biasing PWV estimates from either AIRS or AMSR-E in the moist tropics. Whether some, infrequent equatorial scenes lead to identical biases in AIRS and AMSR-E is a question for future work. Such a study will require a larger set of radiosondes than the ~ 100 examined by Tobin *et al.* [2006].

[49] As discussed earlier, the AIRS full retrievals are validated against radiosondes, but AMSR-E has not been completely validated. Shortcomings in the AMSR-E methodology offer a plausible explanation for some of the biases seen here. Biases can be introduced into AMSR-E by several mechanisms, including an incomplete training ensemble for its regression algorithm, and PWV cross contamination by clouds, rain, or wind-induced surface roughness. The AMSR-E water vapor regression retrieval uses a set of 42,000 radiosondes from island sites for training and evaluation [Wentz and Meisner, 2000]. These include a wide range of oceanic conditions; large AMSR-E biases are avoided by frequently updating the regression coefficients. One exception is stratus formed under warm, dry atmospheric conditions immediate west of Peru, Baja, California, or Namibia during summer. Most other stratus locations are well sampled, including those with cooler air and sea temperatures [Klein and Hartmann, 1993]. Two island sites east of Japan are included in the AMSR-E sonde set, sampling the cold air outbreaks adjacent to (but not in) a region where biases in Figure 8 are seen to be largest. An incomplete AMSR-E training set therefore could explain part of the wet bias in AIRS in the northeast Pacific or in subtropical stratus belts immediately adjacent to continents.

[50] A simple way to test whether microwave soundings techniques lead to dry biases in stratus regions is by examining biases in AIRS full retrievals relative to AIRS partial retrievals. This comparison treats AMSU and HSB as another microwave sounding system. (Note that AMSU/HSB retrievals are based on a physical model while AMSR-E uses radiosonde-based regression. These techniques are two distinct ways to reach a PWV estimate.) AMSR/HSB gives results similar to those seen in Figure 8, including the wet maxima in stratus regions. This supports our contention that AIRS full retrievals are biased relative to AMSR-E because of cloud-induced sampling effects, not because of significant biases in AMSR-E. AMSR-E PWV cross contamination by clouds, precipitation or wind could also account for part of the biases seen here, especially at high latitudes. However, cross contamination is unlikely to explain the shift in sign of biases across the north Pacific

seen in Figure 8 since cloud amount, precipitation and wind speeds are all large across the entire Pacific Ocean basin in winter. Also, the AMSR-E sonde training set is well represented over oceanic middle latitudes. In summary, biases in AMSR-E PWV may explain a small portion (5–10%) of AIRS-AMSR-E total biases discussed in this study. However, the effects of clouds on AIRS full retrieval sampling most plausibly explain biases of 15–70% absolute, as seen in some regions.

[51] The results shown here have important ramifications for height-dependent climatologies from AIRS. Those climatologies must utilize the full retrievals, so any sampling biases in the PWV also likely affect the profile quantities. A significant sampling bias can be expected in high-latitude storm system, where we anticipate clouds lead to climatologies too dry by as much as 30%, at least in the lowest layers dominating the PWV. Similarly, we can expect the AIRS height-resolved water vapor climatologies in stratus regions to be moist by 5 to 15% at lower levels. However, even in these regions the AIRS data are well suited to the study of some phenomena, especially those where less cloudy conditions prevail; see Waugh [2005] for one such study. PWV estimates from AIRS are unbiased throughout the tropics, implying that height resolved water vapor there is less affected by sampling biases. The AIRS water vapor results appear best suited to studies of processes in the subtropical trade wind cumulus belts, where PWV is unbiased against AMSR-E, and full retrieval yields are as high as 90%.

[52] While this discussion has focused on the effects of clouds on AIRS retrievals, the combination of AIRS and AMSR-E provides much information about atmospheric water vapor for all conditions except strong precipitation. AMSR-E samples PWV, sea surface temperature and cloud liquid water under most conditions, even where clouds prevent AIRS from retrieving a well-resolved vertical profile. Moreover, the instruments on the Aqua observe clouds in detail. These cloud observations will be instrumental in generating climatologies of AIRS water vapor conditional upon cloud state. An AIRS water vapor climatology presented as means over space and time, but also over a range of cloud fractions (or other cloud parameters), will more completely convey the information content of the AIRS data. These conditional climatologies will address many questions concerning atmospheric water vapor.

[53] Finally, the effects of clouds on AIRS sampling are relevant also to the Cross-Track Infrared and Microwave Sounding Suite (CrIMSS) on the National Polar Orbiting Satellite System. CrIMSS is the next-generational operational sounder, to replace TOVS within the next several years. The CrIMSS specifications are similar to those of AIRS/AMSU/HSB, and CrIMSS will experience similar cloud-induced sampling effects. Those sampling effects must be fully characterized if a decades-long record of atmospheric state is to be generated from the combined AIRS and CrIMSS systems.

[54] **Acknowledgments.** Anonymous reviewers are largely responsible for the strengths and content of this paper. A reviewer of Fetzer *et al.* [2004a] noted the importance of possible AIRS sampling biases. The comments of three anonymous reviewers were especially helpful in strengthening the discussion presented here. Conversations with Evan Fishbein have helped clarify the challenges of cloud-induced sampling in AIRS. AMSR-E data are produced by Remote Sensing Systems and

sponsored by the NASA Earth Science REASoN DISCOVER Project and the AMSR-E Science Team. Data are available at <http://www.remss.com>. This work was performed at the Jet Propulsion Laboratory, California Institute of Technology, under contract with NASA.

References

- Amenu, G. G., and P. Kumar (2005), NVAP and reanalysis-2 global precipitable water vapor products, *Bull. Am. Meteorol. Soc.*, *86*, 245–256.
- Aumann, H. H., et al. (2003), AIRS/AMSU/HSB on the Aqua mission: Design, science objectives, data products and processing system, *IEEE Trans. Geosci. Remote Sens.*, *41*, 253–264.
- Chaboureaud, J. P., A. Chedin, and N. A. Scott (1998), Remote sensing of the vertical distribution of atmospheric water vapor from the TOVS observations: Method and validation, *J. Geophys. Res.*, *103*, 8743–8752.
- Dai, A. G., J. H. Wang, R. H. Ware, and T. Van Hove (2002), Diurnal variation in water vapor over North America and its implications for sampling errors in radiosonde humidity, *J. Geophys. Res.*, *107*(D10), 4090, doi:10.1029/2001JD000642.
- Divakarla, M. G., C. D. Barnet, M. D. Goldberg, L. M. McMillin, E. Maddy, W. Wolf, L. Zhou, and X. Liu (2006), Validation of Atmospheric Infrared Sounder temperature and water vapor retrievals with matched radiosonde measurements and forecasts, *J. Geophys. Res.*, *111*, D09S15, doi:10.1029/2005JD006116.
- Fetzer, E. J., et al. (2003), Validation Of AIRS/AMSU/HSB core products for data release version 3.0, August 13, 2003, *JPL D-26538*, 79 pp., NASA Goddard Space Flight Cent., Greenbelt, Md. (Available at <http://disc.gsfc.nasa.gov/AIRS/index.shtml/>)
- Fetzer, E., J. Teixeira, E. Olsen, and E. Fishbein (2004a), Satellite remote sounding of atmospheric boundary layer temperature inversions over the subtropical eastern Pacific, *Geophys. Res. Lett.*, *31*, L17102, doi:10.1029/2004GL020174.
- Fetzer, E. J., B. A. Kahn, E. T. Olsen, and E. F. Fishbein (2004b), High lapse rates in AIRS retrieved temperatures in cold air outbreaks, paper presented at 13th Conference on Interactions of Sea and Atmosphere, Am. Meteorol. Soc., Portland, Maine.
- Fetzer, E. J., A. Eldering, E. F. Fishbein, T. Hearty, W. F. Irion, and B. Kahn (2005), Validation Of AIRS/AMSU/HSB core products for data release version 4.0, March 8, 2005, *JPL D-31448*, 79 pp., NASA Goddard Space Flight Cent., Greenbelt, Md. (Available at <http://disc.gsfc.nasa.gov/AIRS/index.shtml/>)
- Froidevaux, L., et al. (2006), Early validation analyses of the atmospheric profiles from EOS MLS on the Aura satellite, *IEEE Trans. Geosci. Remote Sens.*, in press.
- Gettelman, A., et al. (2004), Validation of satellite data in the upper troposphere and lower stratosphere with in situ aircraft instruments, *Geophys. Res. Lett.*, *31*, L22107, doi:10.1029/2004GL020730.
- Iskenderian, H. (1995), A 10-year climatology of Northern Hemispheric tropical cloud plumes and their composite flow patterns, *J. Clim.*, *8*, 1630–1637.
- Kawanishi, T., T. Sezai, Y. Ito, K. Imaoka, T. Takeshima, Y. Ishido, A. Shibata, M. Miura, H. Inahata, and R. W. Spencer (2003), The Advanced Microwave Scanning Radiometer for the Earth Observing System (AMSR-E), NASA's contribution to the EOS for global energy and water cycle studies, *IEEE Trans. Geosci. Remote Sens.*, *41*, 184–194.
- King, M. D., R. Greenstone, and W. Bandeen (Eds.) (1999), *EOS Science Plan: The State of Science in the EOS Program*, 397 pp., NASA Goddard Space Flight Cent., Greenbelt, Md.
- Klein, S. L., and D. L. Hartmann (1993), The seasonal cycle of low stratiform clouds, *J. Clim.*, *6*, 1587–1606.
- Lambrigtsen, B. H. (2003), Calibration of the AIRS microwave instruments, *IEEE Trans. Geosci. Remote Sens.*, *41*, 369–378.
- Lambrigtsen, B. H., and R. V. Calheiros (2003), The humidity sounder for Brazil—An international partnership, *IEEE Trans. Geosci. Remote Sens.*, *41*, 352–361.
- Lambrigtsen, B. H., and S.-Y. Lee (2003), Coalignment and synchronization of the AIRS instrument suite, *IEEE Trans. Geosci. Remote Sens.*, *41*, 343–351.
- McPhaden, M. J. (2004), Evolution of the 2002/03 El Niño, *Bull. Am. Meteorol. Soc.*, *85*, 677–695.
- Norris, J. R. (1998), Low cloud type over ocean from surface observations. Part I: Relationship to surface meteorology and the vertical distribution of temperature and moisture, *J. Clim.*, *11*, 369–382.
- O'Neill, L. L., D. B. Chelton, S. K. Esbensen, and F. F. Wentz (2005), High-resolution satellite measurements of the atmospheric boundary layer response to SST variations along the Agulhas return current, *J. Clim.*, *18*, 2706–2723.
- Pagano, T. S., H. H. Aumann, D. E. Hagan, and K. Overoye (2003), Pre-launch and in-flight radiometric calibration of the Atmospheric Infrared Sounder (AIRS), *IEEE Trans. Geosci. Remote Sens.*, *41*, 265–273.
- Parkinson, C. L. (2003), Aqua: An Earth-observing satellite mission to examine water and other climate variables, *IEEE Trans. Geosci. Remote Sens.*, *41*, 173–183.
- Pyatt, H. E., B. A. Albrecht, C. Fairall, J. E. Hare, N. Bond, P. Minnis, and J. K. Ayers (2005), Evolution of marine atmospheric boundary layer structure across the cold tongue-ITCZ complex, *J. Clim.*, *18*, 737–753.
- Ralph, F. M., P. J. Neiman, and G. A. Wick (2004), Satellite and CALJET aircraft observations of atmospheric rivers over the eastern North Pacific ocean during the winter of 1997/98, *Mon. Weather Rev.*, *132*, 1721–1745.
- Randel, D. L., T. H. vonder Haar, M. A. Ringerud, G. L. Stephens, T. J. Greenwald, and C. L. Combs (1996), A new global water vapor dataset, *Bull. Am. Meteorol. Soc.*, *77*, 1233–1246.
- Rosenkranz, P. W. (2003), Rapid radiative transfer model for AMSU/HSB channels, *IEEE Trans. Geosci. Remote Sens.*, *41*, 362–368.
- Shibata, A., K. Imaoka, and T. Koike (2003), AMSR/AMSR-E level 2 and 3 algorithm developments and data validation plans of NASDA, *IEEE Trans. Geosci. Remote Sens.*, *41*, 195–203.
- Stephens, G. L., et al. (2002), The Cloudsat mission and the A-train—A new dimension of space-based observations of clouds and precipitation, *Bull. Am. Meteorol. Soc.*, *83*, 1771–1790.
- Stevens, B., et al. (2003), Dynamics and chemistry of marine stratocumulus—DYCOMS-II, *Bull. Am. Meteorol. Soc.*, *84*, 579–593.
- Susskind, J., C. D. Barnet, and J. M. Blaisdell (2003), Retrieval of atmospheric and surface parameters from AIRS/AMSU/HSB data in the presence of clouds, *IEEE Trans. Geosci. Remote Sens.*, *41*, 390–409.
- Susskind, J., C. Barnet, J. Blaisdell, L. Iredell, F. Keita, L. Kouvaris, G. Molnar, and M. Chahine (2006), Accuracy of geophysical parameters derived from Atmospheric Infrared Sounder/Advanced Microwave Sounding Unit as a function of fractional cloud cover, *J. Geophys. Res.*, doi:10.1029/2005JD006272, in press.
- Szczodrak, M., P. J. Minnett, and C. Gentemann (2006), Comparison of AMSR-E retrievals of total water vapor over the ocean with ship based measurements, paper presented at 10th Symposium on Integrated Observing and Assimilation Systems for the Atmosphere, Oceans, and Land Surface (IOAS-AOLS), Am. Meteorol. Soc., Atlanta, Ga. (Available at http://ams.confex.com/ams/Annual2006/techprogram/paper_105174.htm)
- Tobin, D. C., H. E. Revercomb, R. O. Knuteson, B. M. Lesht, L. L. Strow, S. E. Hannon, W. F. Feltz, L. A. Moy, E. J. Fetzer, and T. S. Cress (2006), Atmospheric Radiation Measurement site atmospheric state best estimates for Atmospheric Infrared Sounder temperature and water vapor retrieval validation, *J. Geophys. Res.*, *111*, D09S14, doi:10.1029/2005JD006103.
- Trenberth, K. E., J. Fasullo, and L. Smith (2005), Trends and variability in column-integrated atmospheric water vapor, *Clim. Dyn.*, *24*, 741–758.
- Waugh, D. W. (2005), Impact of potential vorticity intrusions on subtropical upper tropospheric humidity, *J. Geophys. Res.*, *110*, D11305, doi:10.1029/2004JD005664.
- Wentz, F. J. (1997), A well-calibrated ocean algorithm for special sensor microwave/imager, *J. Geophys. Res.*, *102*, 8703–8718.
- Wentz, F. J., T. Meisner (2000), Algorithm theoretical basis document version 2: AMSR ocean algorithm, NASA Goddard Space Flight Cent., Greenbelt, Md. (Available at http://eosps.gsf.nasa.gov/eos_homepage/for_scientists/atbd/)
- Wentz, F. J., C. Gentemann, and P. Ashcroft (2003), On-orbit calibration of AMSR-E and the retrieval of ocean products, paper presented at 12th Conference on Satellite Meteorology and Oceanography, Am. Meteorol. Soc., Long Beach, Calif.
- Wittmeyer, I. L., and T. H. vonder Haar (1994), Analysis of the global ISCCP TOVS water vapor climatology, *J. Clim.*, *7*, 325–333.
- Wu, X. Q., J. J. Bates, and S. J. S. Khalsa (1993), A climatology of the water vapor band brightness temperatures from NOAA operational satellites, *J. Clim.*, *6*, 1282–1300.

H. H. Aumann, M. T. Chahine, A. Eldering, E. J. Fetzer, and B. H. Lambrigtsen, Jet Propulsion Laboratory, California Institute of Technology, Pasadena, CA 91109, USA. (eric.j.fetzer@jpl.nasa.gov)